Prognostication of LED Remaining Useful Life and Color Stability in the Presence of Contamination

Pradeep Lall
Auburn University
Department of Mechanical Engineering and
NSF CAVE3 Electronics Research Center
Auburn, AL 36849
Tele:(334)844-3424
E-mail:lall@auburn.edu

Hao Zhang
Auburn University
Department of Mechanical Engineering and
NSF CAVE3 Electronics Research Center
Auburn, AL 36849

Lynn Davis
RTI International
Research Triangle Park, NC 27709

Abstract*— The reliability of LED products may be affected by both luminous flux drop and color shift. Previous research on the topic focuses on either luminous maintenance or color shift. However, luminous flux degradation usually takes very long time to observe in LEDs under normal operating conditions. In this paper, the impact of a VOC (volatile organic compound) contaminated luminous flux and color stability are examined. As a result, both luminous degradation and color shift had been recorded in a short time. Test samples are white, phosphor-converted, high-power LED packages. Absolute radiant flux is measured with integrating sphere system to calculate the luminous flux. Luminous flux degradation and color shift distance were plotted versus aging time to show the degradation pattern. A prognostic health management (PHM) method based on the state variables and state estimator have been proposed in this paper. In this PHM framework, unscented kalman filter (UKF) was deployed as the carrier of all states. During the estimation process, third order dynamic transfer function was used to implement the PHM framework. Both of the luminous flux and color shift distance have been used as the state variable with the same PHM framework to exam the robustness of the method. Predicted remaining useful life is calculated at every measurement point to compare with the tested remaining useful life. The result shows that state estimator can be used as the method for the PHM of LED degradation with respect to both luminous flux and color shift distance. The prediction of remaining useful life of LED package, made by the states estimator and data driven approach, falls in the acceptable error-bounds (20%) after a short training of the estimator.

Keywords- Light emitting diode, Color Stability, VOCs contamination, Accelerated Test

I. Introduction

White LED products have various advantages compared with traditional incandescent lamp or compact fluorescent lamp. They are becoming more and more popular in the general illumination application, because of its high efficiency, long life hours, high programmable switch speed, and various colors. Previous study shows that luminous flux degradation and color shift are the most important failure mechanism of bare LED. According to the manufactures, the lifetime of LED system can be as long as 25000hours. However, the presence of incompatible volatile organic compounds during the assemble process of illumination system can impair both the color and luminous flux output in a very short time at harsh environment [1]. The lifetime under contamination environment can drop to 200hours from the accelerated life test experiment. Also, the color quality of the illumination system can shift dramatically in a short time. The shift of chromaticity coordinates and degradation of luminous flux help to build the PHM framework of the LED package. The data driven approach has been used in the PHM framework, since the failure governing equation based on the physics has not been obtained yet. The analysis of experimental data of luminous flux and chromaticity coordinates helps driven the state vector forward to get the predicted future states. Remaining useful life (RUL) can be calculated based the failure threshold and prediction of future states. Predictions of RUL can be compared with the experimental data to exam the robustness of the estimator. Luminous flux and color shift distance are the measured variables and the real output of the LED system. Estimator utilize them to estimate the state of the LED system. The presented method can be employed to predict the failure of LED caused by thermal and humid stresses. During the aging test of this paper, highly accelerated lift test also known as the "Hammer Test" had been performed on the bare LED test samples. LED samples were connected in series and subject to wet high temperature operational life test (WHTOL). At the same time, samples were subjected to power cycle at constant current 350mA at an interval of one hour. Failure of the LEDs happened due to the contamination source and harsh test

978-1-4799-1894-2/15/$31.00 ©2015 IEEE

environment. The result shows that the contamination caused by VOC material can impair the lifetime of LED packages dramatically and the contamination process is reversible if samples are transferred to clean environment. There is no damage of the chips, phosphor during the contamination process.

II. VOC CONTAMINATION THEORY

LED products usually are systems and have various parts working together. Edison Screw socket play a role of outlet of LED product to connect the driver with the mainline power in the wall. It has the same standard with existing incandescent lamp and compact fluorescent lamps and makes it easy for LED products to replace the incandescent lamp. Most of the LED product has some plastic, glass, or ceramic surroundings connected with the Edison screw socket to seal the whole system, which makes the product much more compact and reliable. During the assemble process of LED-based lamp, a lot of connectors and compounds are used to connect all these parts. Glues, screws, washers, compounds are all potential contaminate source which will lay off VOC at high temperature and harsh working environment. As a result, they will impair the luminous flux output and the chromaticity coordinate of LED products. The majority of white light LED packages use the combination of blue LED chip and yellow down convert phosphor. The remix of yellow light and blue light give the appearance of white light. The phosphor layer is the blender of phosphor powder and silicone polymer. Silicone polymers is a very widely used material during the design of LED based products. It has excellent light transmittance characteristics: stable over wide temperature ranges, resistant to yellowing due to ultraviolet exposure.

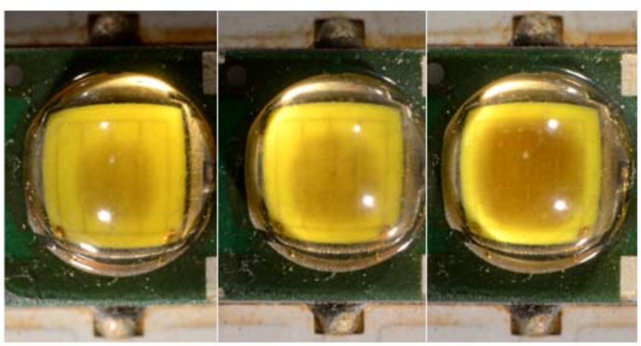

Figure 1 Appearance of Contaminated LED Package

The basic structure of LED's lens, encapsulations, phosphor binder is silicone polymer which is a stable chemical compound. Silicone polymers have very good moisture and gas permeability. Due to the material properties of silicone, VOC can diffuse into silicone lens, encapsulation of LED, and the binder of phosphor. As a result, VOCs will occupy the free space in the interwoven of silicone polymer. With subsequent exposure to high photon energy emitted from the LED chips, along with the heat from the LED die, the VOC sitting inside the silicone polymer can discolor. All the contamination results show that the discolor starts from the center of the chip and contamination area is symmetric, because the center point of the chip has the highest temperature. Figure 1 shows the typical appearance and propagation of a contaminated LED package.

III. EXPERIMENTAL SETUP

Test samples are subjected to both thermal and relative humidity stress in a contaminated chamber. The accelerated test temperature is 85°C and the relative humidity is 85%. During the test, LED modules were power cycled at one hour interval. The readout time interval is 168hours (one week). At each measurement time, LED modules were taken out of the chamber and cool down to room temperature. After the test, they were attached to the heat sink again and moved back to the chamber. At the readout time, LED modules was removed from the heat sink and mounted on a fin heat sink which helps lower the junction temperature during the test in the integrating sphere. Luminous flux, chromaticity coordinate, color temperature are recoded at each time for the future study of the color shift. The measurement forward current is 1000mA and the power cycled forward current is 350mA.

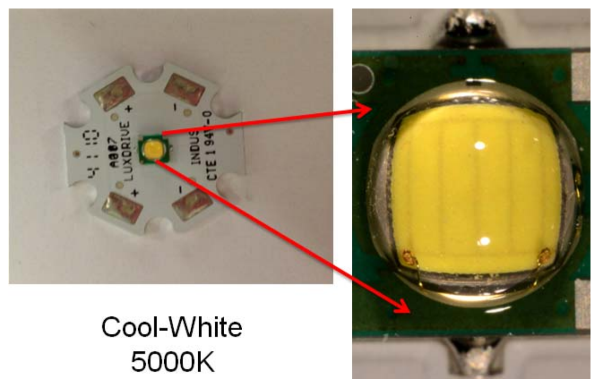

Figure 2 Test Sample

Figure 3 Test Setup in the Chamber

The maximum forward current of the test lamp is 1500mA and both performed current is among the functional range according to the datasheet. In order to record the discolor process under the contamination environment, pictures of the LED modules lens and phosphor are taken. Figure 2 shows the test sample and characteristics. From the picture, wire bond, phosphor layer can be seen clearly. Figure 3 shows the test set up inside of temperature and relative humidity chamber.

IV. TEST RESULT

Figure 4 and Figure 5 show the luminous flux and color shift distance test result in the contaminated chamber. The test result shows that VOC discoloration shifts the LED chromaticity coordinate and degrade the luminous flux in a short time.

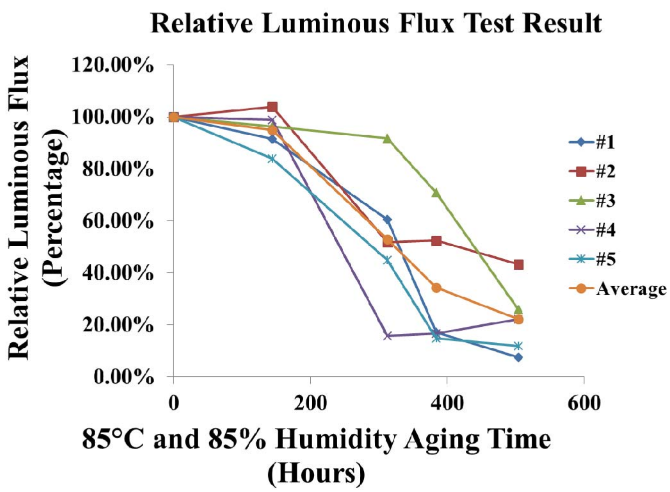

Figure 4 Relative Luminous Flux

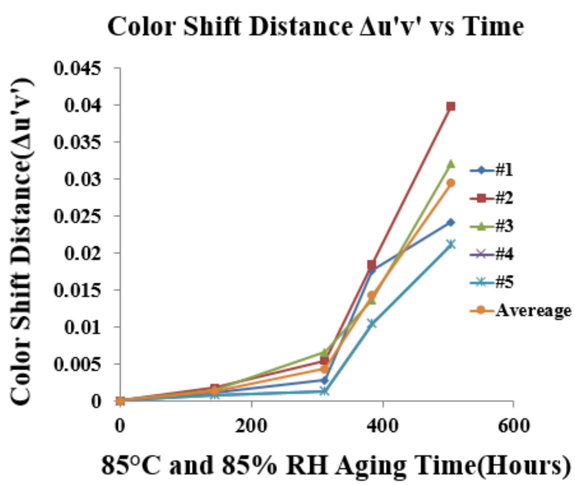

Figure 5 Color Shift Distance

V. STATE ESTIMATION FRAMEWORK

The State Estimation method includes both discrete time state estimation and continuous time state estimation. In this paper, discrete time estimation has been adopted and discussed. In control theory, a state observer is algorithm that provides an estimate of the internal state of a given real system, from measurements of the input and output of the real system. The basic framework of discrete state estimation looks like the following Figure 6.

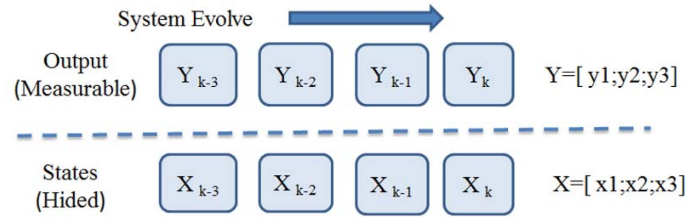

Figure 6 State Estimation Framework

The mathematical model used in the state estimation usually has two master equations for the discrete state estimation. The first is called state transfer equation and the second is output equation which describes the relationship between the state variables and the output variable.

$$X_k = f(X_{k-1}, U_{k-1}, V_{k-1}) \tag{1}$$

In this equation, X_k is state variable matrix. k stands for current time and k-1 is the previous time. U_{k-1} is the previous step known input to the system and V_{k-1} is the process noise of the mathematical model applied to the practical model.

$$Y_k = h(X_k, U_k, N_k) \tag{2}$$

The output equation has three parameters, state variables, known input, and the measurement noise. In practical situation, X_k represented the unobservable states of the system and Y_k is the observable signal. A lot of state estimation techniques have been developed for now. In this paper, Unscented Kalman Filter as the discrete control method will be employed for the model.

VI. UNSCENTED TRANSFORMATION

Assume state x vector has L variables and goes through a non-linear function y=g(x). The mean of x is $\bar{x}$ and covariance is P_x. To calculate the statics of y, a combined matrix X of 2*L+1sigma state vector x has been created according to the following equation. In the following equation, subscript stands for the column number.

$$\begin{aligned} X_0 &= \bar{x} \\ X_i &= \bar{x} + \left(\sqrt{(L+\lambda) * P_x}\right)_i \quad i=1,2,\ldots L \\ X_i &= \bar{x} - \left(\sqrt{(L+\lambda) * P_x}\right)_i \quad i=L+1,L+2,\ldots 2*L \\ \lambda &= a^2 * (L+k) - L \end{aligned} \tag{3}$$

In the above equation, a variable determines the spread of the sigma points around $\bar{x}$ is usually set to a small positive number. K is a second scaling number which usually set to 0. Different weight factor of each column of the combined matrix have been assigned in the following equation and subscripts stands for the column number.

$$W_0^m = \frac{\lambda}{L+\lambda}$$
$$W_0^c = \frac{\lambda}{L+\lambda} + (1 - a^2 + \beta) \tag{4}$$
$$W_i^m = W_i^c = \frac{1}{2*(L+\lambda)} \quad \text{i=1,2,3,…2*L}$$

In the above equation, β is employed to incorporate prior knowledge of the distribution of x and for Gaussian distribution equals 2. The combined sigma vectors propagate forward through the state transfer equation.

$$Y = g(X) \tag{5}$$

The mean and variance of the y are calculated with the weighting factor W^m and W^c in the following equation.

$$\bar{y} = \sum_{i=0}^{2*L} W_i^m * Y_i \tag{6}$$
$$P_y = \sum_{i=0}^{2*L} W_i^c * \{Y_i - \bar{y}\} * \{Y_i - \bar{y}\}^T$$

The unscented Kalman filter is the recursive expansion of the unscented transformation. The nonlinear function g will be replaced by the state transfer function F. Combined state vector matrix is the unscented transformed previous estimated state X_{k-1} and the output X_k is the next estimated state. From the measurable output signal, the true state variable can be calculated. The following phase describes the UKF state estimation procedures.

VII. UNSCENTED KALMAN FILTER ALGORITHM

The advantage the UKF is unscented transformation which can calculate the statistics of a random variable which undergoes a nonlinear transformation. With a set of carefully chosen sample points and their weight, UKF can capture the true mean and variance of the state variable when it goes through no-linear system. UKF algorithm has advantages compared to other estimator [24]. It is easy to implement and has higher accuracy. Due to the unscented transformation, it consider at least second order Taylor expansion. Also, sigma point sampling is an optimal sampling approach compared with the Monte Carlo random sampling method which used in other estimator. Figure 7 shows the framework of UKF.

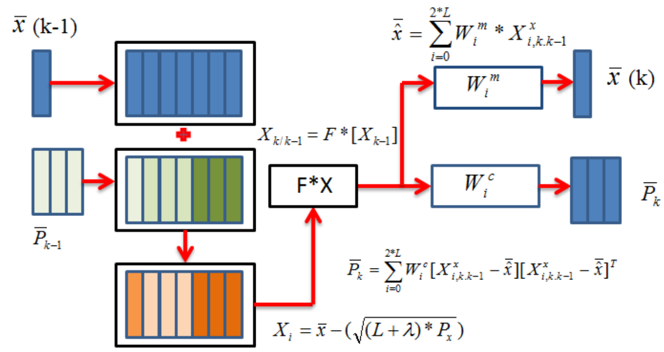

Figure 7 UKF Framework

The UKF algorithm is given in four steps. First, algorithm stars with initialization of state variable at zero time.

$$\hat{x}_0 = E[x_0]$$
$$P_0 = E[(x_0 - \hat{x}_0) * (x_0 - \hat{x}_0)^T] \tag{7}$$

Augment state vector and covariance matrix are followed:

$$\hat{x}_0^a = E[x_0^a] = [\hat{x}_0{}^T \; 0 \; 0]^T$$
$$P_0^a = E[(x_0^a - \hat{x}_0^a) * (x_0 - \hat{x}_0^a)^T] = \begin{bmatrix} P_0 & 0 & 0 \\ 0 & P_v & 0 \\ 0 & 0 & P_n \end{bmatrix} \tag{8}$$

Second, perform unscented transformation and calculate the sigma point:

$$X_{k-1}^a = [\hat{x}_{k-1}^a \quad \hat{x}_{k-1}^a \pm \sqrt{(L+\lambda) * P_{k-1}^a}] \tag{9}$$

Third, time updating according to the state transfer function, updates state variables first, then update output.

$$X_{k/k-1}^a = F * [X_{k-1}^x, X_{k-1}^v] \tag{10}$$
$$\bar{\hat{x}} = \sum_{i=0}^{2*L} W_i^m * X_{i,k.k-1}^x$$
$$\bar{P}_k = \sum_{i=0}^{2*L} W_i^c [X_{i,k.k-1}^x - \bar{\hat{x}}][X_{i,k.k-1}^x - \bar{\hat{x}}]^T$$

Output update

$$Y_{k/k-1} = H * [X_{k-1}^x, X_{k-1}^n] \tag{11}$$
$$\bar{\hat{y}} = \sum_{i=0}^{2*L} W_i^m * Y_{i,k.k-1}^x$$

The last step uses the covariance of output and state variable updates the measurement equation.

$$P_{\bar{\hat{y}},\bar{\hat{y}}} = \sum_{i=0}^{2*L} W_i^c [Y_{i,k.k-1}^x - \bar{\hat{y}}][Y_{i,k.k-1}^x - \bar{\hat{y}}]^T \tag{12}$$

$$P_{\bar{\hat{x}},\bar{\hat{y}}} = \sum_{i=0}^{2*L} W_i^c [X_{i,k.k-1}^x - \bar{\hat{x}}][Y_{i,k.k-1}^x - \bar{\hat{y}}]^T$$

$$K = P_{\bar{\hat{x}},\bar{\hat{y}}} * P_{\bar{\hat{y}},\bar{\hat{y}}}^{-1}$$

$$\hat{x}_k = \bar{\hat{x}} + K * (y_k - \bar{\hat{y}})$$

$$P_k = \bar{P}_k - K * P_{\bar{\hat{y}}*\bar{\hat{y}}} * K^T$$

VIII. PHM FRAMEWORK

Various PHM approaches had been proposed by other researchers for the estimation of unknown states and the prediction of remaining useful life. The very common used one is based on the physical model of failure. The prediction of RUL depends on the mathematical dominant governing equation which describes the physical failure process [2-15]. The second one use state estimator to estimate the true unknown states and predict the RUL based on the parameters got from the estimator [16-19]. There are also some other techniques that use mathematical fitting of the experimental data to get the RUL. However, the fitting method is very sensitive to the experimental value. If the experimental noise is high, the error between the real model and the fitted model will be gigantic. For now, there is not published physics based failure model for LED lumen degradation. In this paper, the state estimator UKF and the data driven technique will be employed to predict the RUL based on the observed luminous flux and color shift distance. The data driven approach relies on the analysis of the in situ monitored data obtained from the experiment. Figure 8 and Figure 9 show the interpolation of the experimental data.

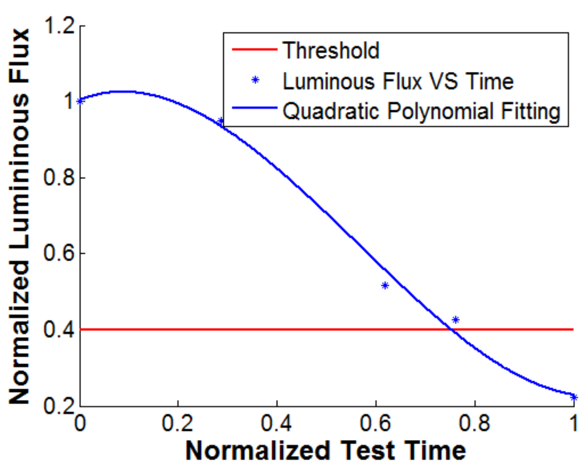

Figure 8 Interpolation of the Measured Luminous Flux

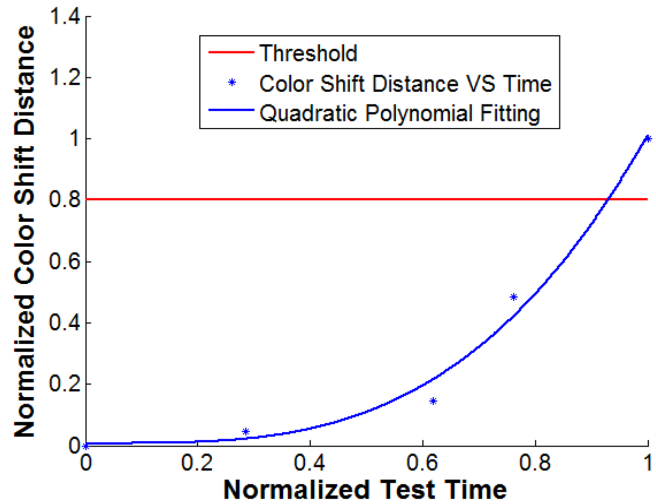

Figure 9 Interpolation of the Measured color Shift Distance

The state estimator estimates the true states under noise and error. After the long enough training, the estimator can works independently without the measured data. The advantage of the estimator over other techniques is the no need for the specified dominant model from the undying physics. Generally, physics model of a technique comes after the techniques become popular. This time gap stops engineers doing the PHM work of products based on the physics model. However, with estimator and the data driven approach, a very short experiment data can train the estimator and make it work stably. The predicted remaining useful life at a specific time consists of two parameters. The first is the mean value and the second value is the confidence interval around the predicted mean value. The predicted end of life, combined with the confidence interval allows statistically decision to be made about the maintenance and use of the system. In prediction, a lot uncertainty involved. Usually, this uncertainty has different distribution. Guassian distribution is the one often used, since a lot of things in nature follow Gaussion distribution. In the beginning, a pseudo model was developed from the measured luminous flux to get some understanding of the pattern. From the test result, it is obvious that quadratic polynomial fits the experimental data very well. Therefore, A Fourth order transfer function was used in the estimator. From the transfer function, there are no specific data for each term. It works for any forth order function and that is beauty of state estimator. There is no need to identify the details of the model. The only thing need to do is to find the pattern. After a short training of the estimator, it is ready to do the estimation.

The first state variable of the system can be the luminous flux or the color shift distance. The second, the third and the fourth state variables are the first derivative, the second derivative and the third derivative of the picked variable. State transfer function is given below and t is the time interval of the test.

$$\begin{bmatrix} x_1[k+1] \\ x_2[k+1] \\ x_3[k+2] \\ x_4[k+1] \end{bmatrix} = \begin{bmatrix} 1 & t & \frac{t^2}{2} & \frac{t3}{6} \\ 0 & 1 & t & \frac{t^2}{2} \\ 0 & 0 & 1 & t \\ 0 & 0 & 0 & 1 \end{bmatrix} * \begin{bmatrix} x_1[k] \\ x_2[k] \\ x_3[k] \\ x_4[k] \end{bmatrix} \quad (13)$$

It should be noticed that there is not physics model in the transfer function. The expansion of the first state is just the Taylor's expansion to the third derivative. The reason why the fourth order transfer function is picked is based on the pseudo model got from the pattern of observed data. The state estimation is based on the previous state vector, process noise, experimental noise, transfer function in the UKF algorithm.

IX. ESTIMATION FOR RUL BASED ON LUMINOUS FLUX AND COLOR SHIFT DISTANCE

In the estimation of RUL, both luminous flux and color shift distance had been used with the same estimator. From observation and fitting method, fourth order polynomial fits both the measured data. The only difference is that luminous flux degrade and color shift distance increase with the aging time. However, that does not confused the algorithm, since both of them follow the same dynamic function. The test data from five test periods will be select to train the algorithm and then the prediction of the failure time will be performed without the experimental data. The period was chosen as the 30%, 40%, 50%, 60%, 70% test data of the entire test time. The following **Error! Reference source not found.**Figure 10 and Figure 11 shows the projection data of the algorithm after training. The convergence of the projection can be observed form the following figure for both luminous flux and color shift distance.

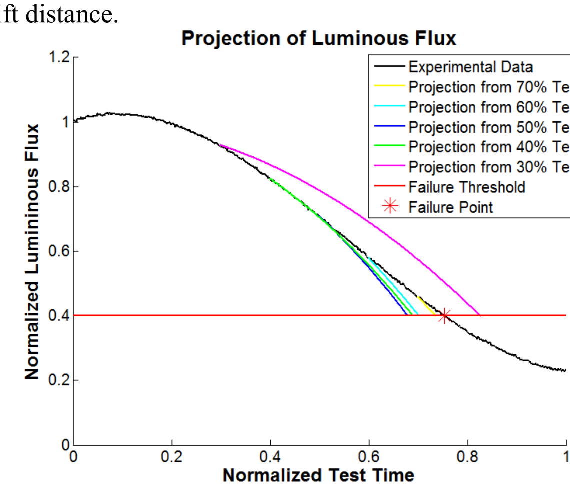

Figure 10 Projection of Luminous Flux with Trained Estimator

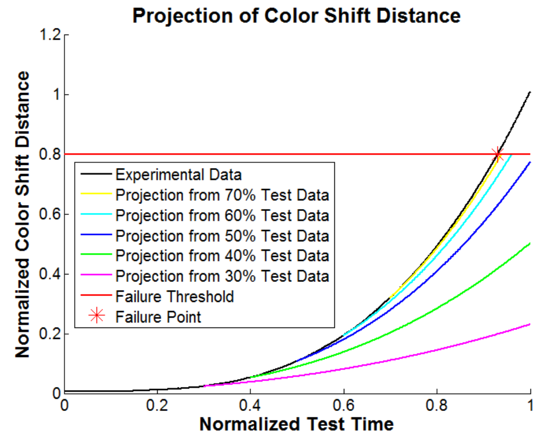

Figure 11 Projection of Color Shift Distance with Trained Estimator

X. PROGNOSTICS METRICS

In order to quantify and validate the PHM method above, a comparison between the observed luminous flux and color shift distance and the predicted values had been done. The validation procedures follow the algorithm assessment metrics proposed in [20-23]. The validation method usually involves four steps. First, calculate the alpha-lambda performance and see whether the prediction converge to the true value. Second, calculate the statistics of the beta equation to see the precision of the algorithm. The third step is to calculate the relative accuracy. The last step of the validation depends on the demands of the algorithm. The alpha-lambda metric compares the actual remaining useful life against the predicted RUL. The actual RUL can be found from the experimental data after the component had been stressed to failure. The alpha bounds are determined by the application and they provide a goal region for the algorithm. In this paper α (±20) % of the actual RUL are chosen. If the predicted RUL falls within the alpha bounds, then it is counted as a correct prediction. It should be noticed that the alpha bounds is different from the confidence interval of the predicted mean value. It defines the acceptable error bound of the prediction. Figure 12 and Figure 13 show the predicted remaining useful life from each test point with the measurement of luminous flux and color shift distance. At the very beginning of the test, approximately 30% of the test time, the algorithm is not able to do the prediction, because the size of the input data is not enough to make the algorithm converge. However, after about the 38 percent of the test time, the algorithm is good enough to make the prediction fall into the 20% boundary of the true remaining useful life. The most important is that, after it falls into the 20% boundary, it does not go out of the boundary which means that the algorithm converges.

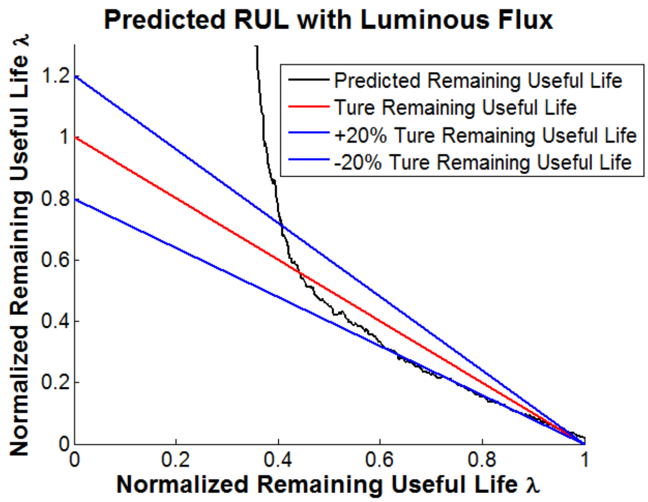

Figure 12 Predicted RUL with Luminous Flux

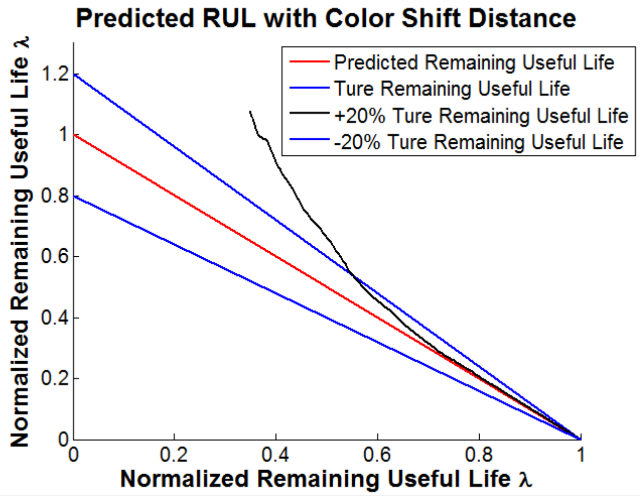

Figure 13 Predicted RUL with Color Shift Distance

In the prediction, all the time value had been normalized by the failure time. In the picture, λ is defined as the normalized time and it can be calculated by t/t_f where f stands for failure. Normalized time is plotted on the x-axis. When lambda equals 0, the part is pristine and when lambda is equal to 1, the part fails.

Beta metric is the second criteria and is defined as how much of the area under the probability density function falls within the alpha bounds at each specific time. With this definition, it can be calculated by the following equation.

$$\beta = \int_{-a}^{+a} p(RUL(t) \mid z_{0:t})dt \tag{14}$$

Since the probability density function defines the distribution of the predicted remaining useful lift, the more area fall into the alpha boundary, the more confidence of the prediction. The whole property density function falls into the 20% boundary when beta equals1.The following Figure 14 shows the beta metric of the algorithm. After the convergence of the algorithm, the beta values jumps around 1.

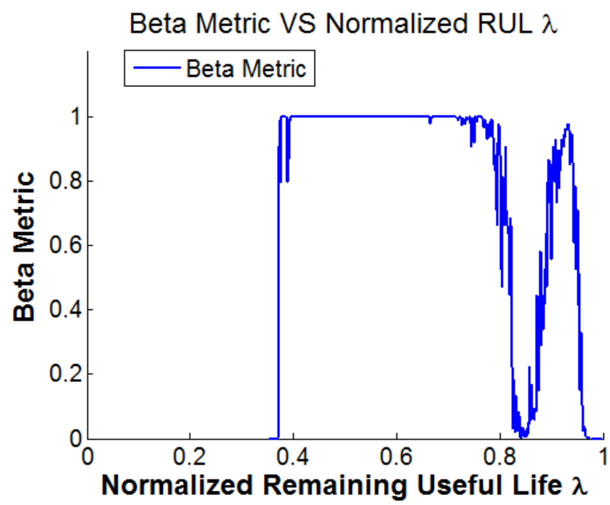

Figure 14 Beta Matric

Relative accuracy is defined as a metric to indicate how closer the predicted remaining useful life to the actual remaining useful life. It can be calculated by the following equation.

$$RA_{\lambda} = 1 - \mid RUL_{actual} - RUL_{predicted} \mid / RUL_{actual} \tag{15}$$

From the equation, relative accuracy equals 1 when predicted value is equal to the true state. The following Figure 15 shows the calculated relative accuracy of the prediction result. The relative accuracy of the algorithm is very close to one after the convergence of the algorithm. It can also be seen from the prediction of the remaining useful life in Figure 15.

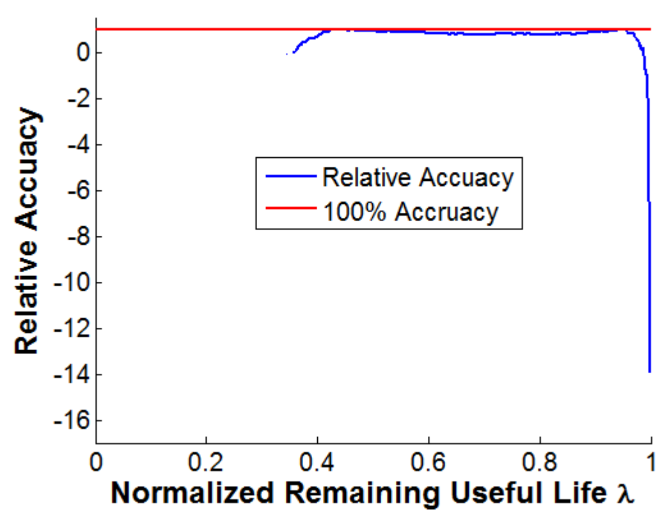

Figure 15 Relative Accuracy of Prediction

In order to summarize the result of the prognostic algorithm into a single function, the performance function used the average Beta metric value and Relative accuracy value. Different weight of them can be assigned based on the demand. Taking the performance function as an equal weight of both accuracy and the RA metric is usually utilized.

XI. CONCLUSION

A PHM approach has been developed based on the state vector of measurement and the estimator. Even the physics based failure model has not established, the measured luminous flux and color shift distance can be used to train the state estimator and predict the state in the future. During the prediction part, the estimated state vector is projected forward based on the dynamic function to predict the remaining useful life based on the picked threshold. According to the simulated result, in order to make the PHM framework work, at least 38% percent experimental data should be measured to train the estimator algorithm. After the training process, the algorithm can work independently to project the state forward and predict the remaining useful life. The result shows that all prediction result can fall into the 20% boundary of the goal. In conclusion, the UKF based PHM framework can be used to predict the remaining useful life of LED products under harsh and contaminated environment based on the measurement of luminous flux or color shift distance.

ACKNOWLEDGMENT

The work presented here in this paper has been supported by a research grant from the Department of Energy under Award Number DE-EE0005124.

REFERENCES

[1] Cree XLamp LEDsChemical Compatibility, Cree, Inc., Durham, NC. , CLD-AP63 rev 4 August, 2013.

[2] Bagul, Y.G., I. Zeid, and S.V. Kamarthi, A Framework for Prognostics and Health Management of Electronic Systems, IEEE Aerospace Conference, pp. 1-9, March 1-8, 2008.

[3] Lall, P., Choudhary, P., Gupte, S., Suhling, J., Health Monitoring for Damage Initiation and Progression during Mechanical Shock in Electronic Assemblies, IEEE Transactions on Components and Packaging Technologies, Vol. 31, No. 1, pp. 173-183, March 2008a.

[4] Lall, P., Panchagade, D., Choudhary, P., Gupte, S., Suhling, J., Failure-Envelope Approach to Modeling Shock and Vibration Survivability of Electronic and MEMS Packaging, IEEE Transactions on Components and Packaging Technologies, Vol. 31, No. 1, pp. 104-113, March 2008b.

[5] Lall, P., Hande, M., Bhat, C., More, V., Vaidya, R., Suhling, J., Algorithms for Prognostication of Prior Damage and Residual Life in Lead-Free Electronics Subjected to Thermo-Mechanical Loads, Proceedings of the 10th Intersociety Thermal and Thermo-mechanical Phenomena (ITherm), Orlando, Florida, pp. 638-651, May 28-31, 2008c.

[6] Lall, P., Bhat, C., Hande, M., More, V., Vaidya, R, Pandher, R., Suhling, J., Goebel, K., Interrogation of System State for Damage Assessment in Lead-free Electronics Subjected to Thermo-Mechanical Loads, Proceedings of the 58th Electronic Components and Technology Conference (ECTC), Orlando, Florida, pp. 918-929, May 27-30, 2008d.

[7] Lall, P., Iyengar, D., Shantaram, S., S., Gupta, P., Panchagade, D., Suhling, J., KEYNOTE PRESENTATION: Feature Extraction and Health Monitoring using Image Correlation for Survivability of Leadfree Packaging under Shock and Vibration, Proceedings of the 9th International Conference on Thermal, Mechanical, and Multi-Physics Simulation and Experiments in Micro-Electronics and Micro-Systems (EuroSIME), Freiburg, Germany, pp. 594-608, April 16-18, 2008e.

[8] Lall, P., Iyengar, D., Shantaram, S., Pandher, R., Panchagade, D., Suhling, J., Design Envelopes and Optical Feature Extraction Techniques for Survivability of SnAg Leadfree Packaging Architectures under Shock and Vibration, Proceedings of the 58th Electronic Components and Technology Conference (ECTC), Orlando, Florida, pp. 1036-1047, May 27-30, 2008f.

[9] Lall, P., R. Lowe, and K. Goebel, Resistance spectroscopy-based condition monitoring for prognostication of high reliability electronics under shock-impact, 59th Electronic Components and Technology Conference, San Diego, CA, pp. 1245-1255, 2009a.

[10] Lall, P., Lowe, R., Suhling, J., Prognostication Based On Resistance-Spectroscopy For High Reliability Electronics Under Shock-Impact, ASME IMECE, pp. 1-12, Lake Buena Vista, FL, Nov 13-19, 2009b.

[11] Lall, P., Lowe, R., Goebel, K., Prognostics Using Kalman-Filter Models and Metrics for Risk Assessment in BGAs Under Shock and Vibration Loads, 60th ECTC, Las Vegas, Nevada, pp. 889-901, June 1-4, 2010a.

[12] Lall, P., Lowe, R., Goebel, K., Use of Prognostics in Risk-Based Decision Making for BGAs under Shock and Vibration Loads, 11th ITHERM, Las Vegas, NV, pp. 1-11, June 2-5, 2010b.

[13] Saha, B. and K. Goebel, Modeling Li-ion Battery Capacity Depletion in a Particle Filtering Framework, Proceedings of the Annual Conference of the Prognostics and Health Mngt Society, http://www.phmsociety.org/node/167, San Diego, CA, pp. 1-10, 2009a.

[14] Saha, B., Prognostics Methods for Battery Health Monitoring Using a Bayesian Framework, , IEEE Transactions on Instrumentation and Measurement, Vol. 58, No. 2, pp. 291-296, 2009b

[15] Saha, B., and K. Goebel, Uncertainty Management for Diagnostics and Prognostics of Batteries using Bayesian Techniques, Proceedings of the IEEE Aerospace Conference, Big Sky, MT, pp. 1-10, March 1-8, 2008.

[16] Swanson, D.C., A General Prognostic Tracking Algorithm for Predictive Maintenance, IEEE Proceedings on Aerospace Conference, Vol. 6, pp. 2971-2977, 2001.

[17] Swanson, David, Michael Spencer, and Sevag Arzoumaniana, Prognostic Modeling of Crack Growth in a Tensioned Steel Band, Mechanical System

[18] Batzel, T.D., and D.C. Swanson, Prognostic Health Management of Aircraft Power Generators, IEEE Transactions on Aerospace and Electronic Systems, Vol. 45, No. 2, pp. 473-482, 2009.

[19] Orchard, M. E, G. J Vachtsevanos, A Particle Filtering Approach for On-Line Failure Prognosis in a Planetary Carrier Plate, International Journal of Fuzzy Logic and Intelligent Systems, Vol. 7, No. 4, 221–227, 2007.

[20] Saxena, A., J. Celaya, B. Saha, S. Saha, and K. Goebel, Evaluating Algorithm Performance Metrics Tailored for Prognostics, IEEE Aerospace Conference, Big Sky, MT, pp. 1-11, March 2008a.

[21] Saxena, A., J. Celaya, E. Balaban, K. Goebel, B. Saha, S Saha, and M. Schwabacher, Metrics for Evaluating Performance of Prognostic Techniques, Intl. Conf. on Prognostics and Health Management, Denver, Colorado, pp. 1-17, October 2008b.

[22] Saxena, A., Celaya, J., Saha, B., Goebel, K., Evaluating algorithm performance metrics tailored for prognostics. IEEE Aerospace conference, 2009a.

[23] Saxena, A., Celaya, J., Saha, B., Saha, S., Goebel, K., On Applying the Prognostics Performance Metrics, Annual Conference of the PHM Society, vol 1, San Diego, CA, 2009b.

[24] Eric A. Wan and Rudolph van der Merwe, The Unscented Kalman Filter for Nonlinear Estimation, Adaptive Systems for Signal Processing, Communications, and Control Symposium 2000. AS-SPCC. The IEEE 2000. Pages 153-158, 01 Oct 2000-04 Oct 2000.